

# Forced synchronization of coupled oscillators

Hiroyuki Kitajima, Yasushi Noumi and Hiroshi Kawakami

*The University of Tokushima, Tokushima, 770 Japan, kitaji@ee.tokushima-u.ac.jp*

**Abstract**— We consider a system of coupled two oscillators with external force. At first we introduce the symmetrical property of the system. When the external force is not applied, the two oscillators are synchronized at the opposite phase. We obtain two different kinds of bifurcation diagrams: the unforced system has (1) stable anti-phase and unstable in-phase solutions and (2) stable anti-phase, unstable in-phase and  $I_{1/2}$ -invariant solutions. We find that the synchronized oscillations eventually become in-phase when the amplitude of the external force is increased.

## I. Introduction

Systems of coupled oscillators have been used extensively in physiological and biochemical modeling studies. Many investigators have been studied two mutually coupled oscillators [1]–[3] because two oscillators' case is a prototype modeling to understand the phenomena in a large number of coupled oscillators. For instance, Kimura et al. investigated synchronization phenomena observed in two oscillators coupled by a resistor with current connection [3]. They confirmed that these oscillators were synchronized at the opposite phase. Using group theoretic discussion applied to the coupled oscillators, we can derive some general theorems concerning with the bifurcations of equilibrium points and periodic solutions [4].

In this study a forced coupled oscillator is analyzed. The dynamics of the circuit becomes invariant under the transformations: (1) interchange of the state variables, and (2) inversion of state variables with time shift  $\pi$  radian [5]. The periodic external force is injected into the invariant subspace of the transformation (1). When the external force is not applied, the two oscillators are synchronized at the opposite phase. We obtain two different kinds of bifurcation diagrams: the unforced system has (1) in-phase and anti-phase solution and (2) in-phase, anti-phase and  $I_{1/2}$ -invariant solution. We find that the synchronized oscillations eventually become in-phase when the amplitude of the external force is increased. The bifurcation processes corresponding to the synchronizations stated above are clarified by the bifurcation diagrams. In the diagram we obtain codimension three bifurcation point of intersection of D-type of branching and Neimark-Sacker bifurcation. Around this point we ob-

serve the bifurcation of quasi-periodic solutions.

## II. Circuit Equation and Related Property

We assume nonlinear conductance  $g(v)$  and voltage source  $e(t)$  in Fig. 1 as

$$g(v) = -a_1 v + a_3 v^3, \quad e(t) = E \sin(\nu t). \quad (1)$$

Then the normalized circuit equations are described by

$$\begin{aligned} \frac{dr_1}{dt} &= -[-c_1 + \frac{c_3}{2}(r_1^2 + 3r_2^2)]r_1 - \omega s_1 - \delta_1 r_1 \\ &\quad + \sqrt{2}\delta_1 B \sin(\nu t) \\ \frac{ds_1}{dt} &= \omega r_1 - \sigma s_1 \end{aligned} \quad (2)$$

$$\begin{aligned} \frac{dr_2}{dt} &= -[-c_1 + \frac{c_3}{2}(3r_1^2 + r_2^2)]r_2 - \omega s_2 - \delta_2 r_2 \\ \frac{ds_2}{dt} &= \omega r_2 - \sigma s_2 \end{aligned}$$

where

$$\begin{aligned} c_1 &= \frac{a_1}{C}, \quad c_3 = \frac{a_3}{C^2}, \quad \sigma = \frac{r}{L}, \quad \omega = \frac{1}{\sqrt{LC}}, \\ B &= \sqrt{C}E, \quad \delta_1 = \frac{G}{C(1+2GG_0)}, \quad \delta_2 = \frac{G}{C}, \\ x_i &= \sqrt{C}v_i, \quad y_i = \sqrt{L}i, \quad (i = 1, 2) \end{aligned}$$

and

$$\begin{aligned} r_1 &= \frac{1}{\sqrt{2}}(x_1 + x_2), \quad s_1 = \frac{1}{\sqrt{2}}(y_1 + y_2), \\ r_2 &= \frac{1}{\sqrt{2}}(x_1 - x_2), \quad s_2 = \frac{1}{\sqrt{2}}(y_1 - y_2). \end{aligned} \quad (3)$$

Equations (2) have following symmetrical operations:

$$\begin{aligned} \sigma_0 &: R^4 \times R \rightarrow R^4 \times R ; \\ &\quad (r_1 \ s_1 \ r_2 \ s_2 \ \nu t) \mapsto (r_1 \ s_1 \ -r_2 \ -s_2 \ \nu t) \\ I_{1/2} &: R^4 \times R \rightarrow R^4 \times R ; \\ &\quad (r_1 \ s_1 \ r_2 \ s_2 \ \nu t) \mapsto (-r_1 \ -s_1 \ -r_2 \ -s_2 \ \nu t - \pi) \\ \sigma_{1/2} &: R^4 \times R \rightarrow R^4 \times R ; \\ &\quad (r_1 \ s_1 \ r_2 \ s_2 \ \nu t) \mapsto (-r_1 \ -s_1 \ r_2 \ s_2 \ \nu t - \pi) \end{aligned} \quad (4)$$

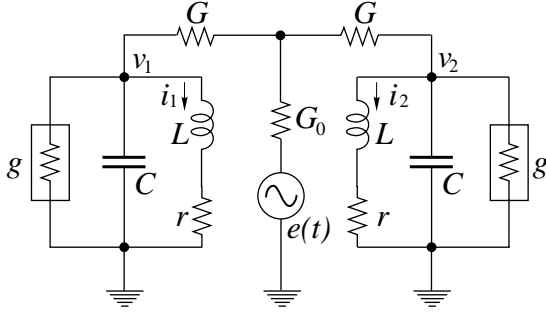


Figure 1: Circuit diagram.

### III. Results

We fix the parameters in Eqs. (2) as

$$c_3 = 1/3, \delta_1 = 1.0, \omega = 1.0, \sigma = 0.5.$$

#### A. Bifurcations of the unforced system

At first we study bifurcations of the unforced system which  $B = 0$  in Eqs. (2). Figure 2 shows a bifurcation diagram of the unforced system. In the shaded region there exists a stable equilibrium point at the origin. Changing the parameters along the curve  $l$ , the first Hopf bifurcation  ${}_0h_2$  and the second Hopf bifurcation  ${}_0h_1$  generate anti-phase and in-phase periodic solution, respectively. The in-phase solution meets the D-type of branching  $D_1$  (symmetry-breaking bifurcation) and generates two  $I_{1/2}$ -invariant solutions [6]. In the next section we consider two cases: the unforced system has (1) anti-phase and in-phase solutions (the point (1) in Fig. 2) and (2) anti-phase, in-phase and  $I_{1/2}$ -invariant solutions (the point (2) in Fig. 2).

#### B. Forced synchronization

##### B.1. case(1)

Figure 3 shows a bifurcation diagram of periodic solutions in Eqs. (2). Because the unforced system ( $B = 0$ ) has anti-phase and in-phase solutions, their corresponding bifurcation sets  $G_1$  and  $G_2$ , and  $G_4$ , respectively, meet the axis of  $B = 0$  at  $\nu_1$  and  $\nu_2$ . Here we are interested in how to change the anti-phase solution under the influence of external force. Figures 4(a)–4(d) show trajectories of the solutions when the amplitude  $B$  of the external force is increased. Note that the external force is applied in-phase direction, see Eqs. (2). When  $B = 0$  the oscillators synchronize at the opposite phase, see Fig. 4(a). Increasing  $B$  two  $I_{1/2}$ -invariant solutions appear (Fig. 4(b) and (c)). If we can find one of them, by the operation  $\sigma_0$  or  $\sigma_{1/2}$  we can easily obtain the other solution. In the

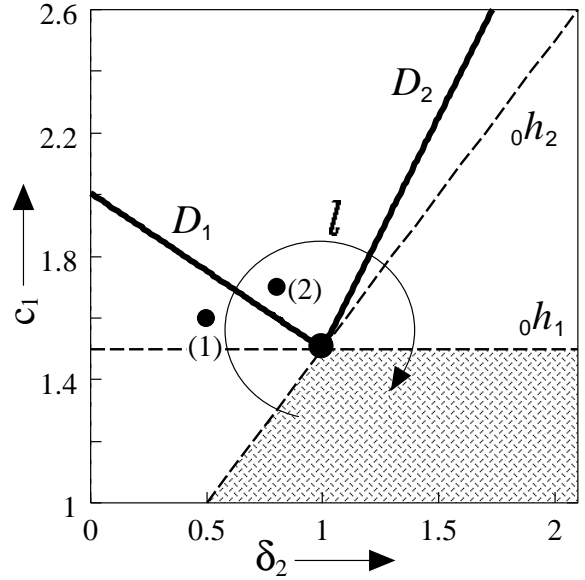


Figure 2: Bifurcation diagram of equilibrium points in Eqs. (2) where  $B = 0$ . Dashed and solid lines indicate Hopf bifurcation of the equilibrium point at the origin and D-type of branching of periodic solutions, respectively.

region these two solutions stably exist. Increasing  $B$  the oscillators synchronize in-phase in the region.

In Fig. 3 open circles indicate the points of intersection of Neimark-Sacker bifurcation set and D-type of branching set of periodic solutions called codimension three bifurcation. Two Neimark-Sacker bifurcation sets  $N_1$  and  $N_2$  (or  $N_3$  and  $N_4$ ) are the bifurcations of different periodic solutions. Changing the parameter along the line  $l_1$  and  $l_2$  two stable and one unstable quasi-periodic solutions are generated, respectively. The two stable solutions are shown in Fig. 5(a) and (b). Decreasing the parameter  $B$  two quasi-periodic solutions become one solutions, see Fig. 5(c). These bifurcation structure is similar to those of  $P^2$ -codimension two bifurcation point[7]. Thus we predict that the large quasi-periodic solution disappear with the quasi-periodic solution generated by  $N_4$ .

##### B.2. case(2)

Figure 6 shows a bifurcation diagram of periodic solutions in Eqs. (2). Because the unforced system ( $B = 0$ ) has anti-phase,  $I_{1/2}$ -invariant and in-phase solutions, their corresponding bifurcation sets  $G_1$  and  $G_2$ ,  $G_5$  and  $G_6$ , and  $G_7$  and  $G_8$ , respectively, meet the axis of  $B = 0$  at  $\nu_1$ ,  $\nu_2$  and  $\nu_3$ . Tangent bifurcation sets  $G_2$  and  $G_3$  are separated and join to D-type of branching at the points of marked by closed circles. Therefore

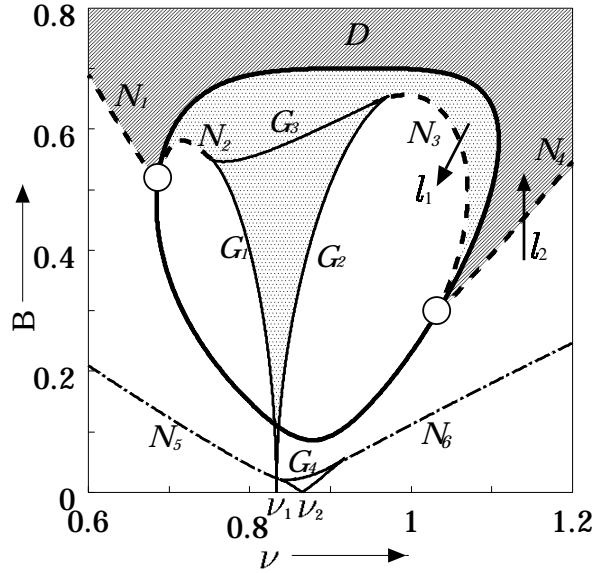


Figure 3: Bifurcation diagram of periodic solutions in Eqs. (2). The symbols  $G$  and  $N$  indicate tangent and Neimark-Sacker bifurcation set, respectively.  $\delta_2 = 0.5$ .  $c_1 = 1.6$ .

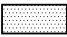
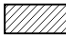
synchronization area  are separated and in the shaded region  two synchronized states are co-exist.

Figure 7 shows a one-parameter bifurcation diagram along the line  $l_3$  in Fig. 6.

#### IV. Concluding Remarks

We have investigated synchronization of coupled two oscillators with external force. When the external force is not applied, the two oscillators are synchronized at the opposite phase. We obtained two different kinds of bifurcation diagrams: the unforced system has (1) anti-phase and in-phase solutions and (2) anti-phase, in-phase and  $I_{1/2}$ -invariant solutions. We found that the synchronized oscillations eventually become in-phase when the amplitude of the external force is increased.

The future problems are to study as follows:

- forced synchronization when the unforced system has different periodic solution,
- the bifurcation of quasi-periodic solutions around the points of intersection of D-type of branching and Neimark-Sacker bifurcation.

#### References

[1] R.H. Rand and P.J. Holmes, "Bifurcation of periodic motions in two weakly coupled van der Pol oscillators," *Int. J. Nonlinear Mech.*, vol.15, pp.387–399, 1980.

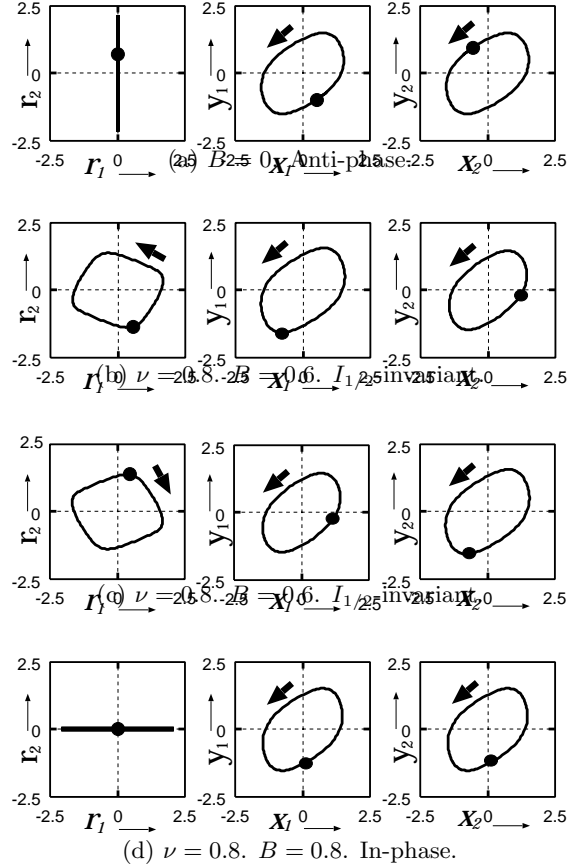


Figure 4: Trajectories of the solutions in Eqs. (2). Arrows and the points marked by closed circles indicate the time direction of the trajectory and the fixed point of Poincaré map, respectively. (Left)  $r_1$  vs.  $r_2$ . (Middle) Oscillator 1. (Right) Oscillator 2.

[2] T. Suezaki and S. Mori, "Mutual synchronization of two oscillators," *IECE*, vol.48, no.9, pp.1551–1557, Sep. 1965.

[3] H. Kimura and K. Mano, "Some properties of mutually synchronized oscillators coupled by resistances," *IECE*, vol.48, no.10, pp.1647–1656, Oct. 1965.

[4] O. Papy and H. Kawakami, "Symmetrical properties and bifurcations of the periodic solutions for a hybrid coupled oscillator," *IEICE Trans.* vol.E78-A, no.12, pp.1816–1821, Dec. 1995.

[5] Y. Noumi and H. Kawakami, "Forced synchronization of coupled oscillators," Technical Report of IEICE, NLP96-172, pp.101–108, March 1997.

[6] H. Kitajima, Y. Noumi, Y. Katsuta and H. Kawakami, "Bifurcation of periodic solutions in a cou-

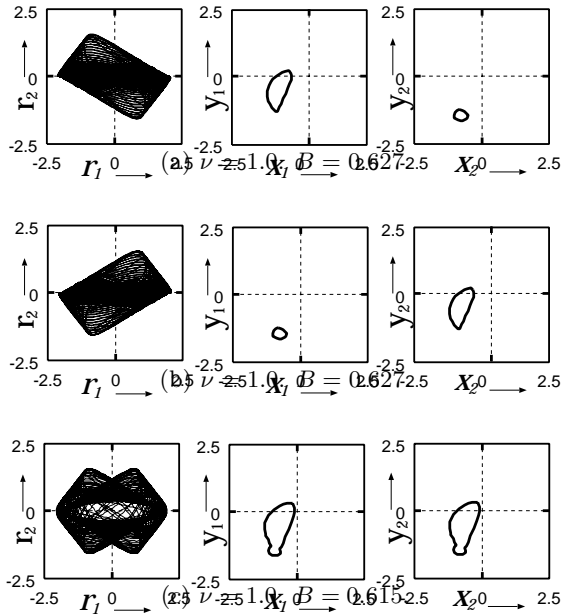


Figure 5: Quasi-periodic solutions in Eqs. (2). (Left) Trajectories.  $r_1$  vs.  $r_2$ . (Middle) The points of Poincaré map for Oscillator 1. (Right) The points of Poincaré map for Oscillator 2.

pled oscillator with voltage ports,” Technical Report of IEICE, NLP97-1, pp.1-8, May 1997.

- [7] H. Kitajima and H. Kawakami, “Cascade of period doubling and Neimark-Sacker bifurcations,” IEICE Trans. vol.J80-A, no.3, pp.491-498, March 1997.
- [8] H. Kawakami, “Bifurcation of periodic responses in forced dynamic nonlinear circuits: computation of bifurcation values of the system parameters,” IEEE Trans. Circuits & Syst., vol.CAS-31, no.3, pp.248-260, March 1984.
- [9] Y. Katsuta, Analysis of symmetrical nonlinear circuit, Doctor thesis, The University of Tokushima, 1995.

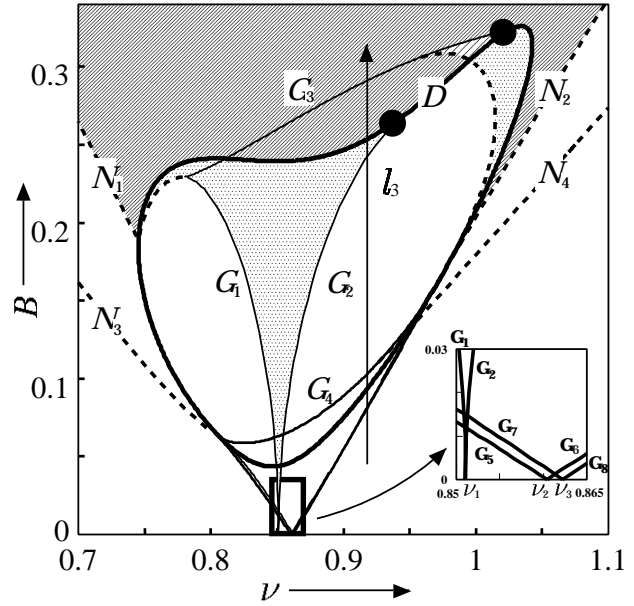


Figure 6: Bifurcation diagram of periodic solutions in Eqs. (2). Small diagram denote the enlarged diagram for small value of  $B$ .  $\delta_2 = 0.8$ .  $c_1 = 1.7$ .

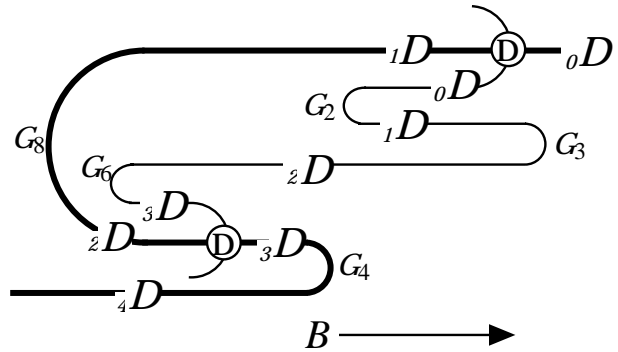


Figure 7: One parameter schematic bifurcation diagram along the line  $l_3$  in Fig. 6. Heavy and light curves indicate the in-phase and  $I_{1/2}$ -invariant solutions, respectively. Subscript of  $D$  represent the dimension of the unstable subspace.  $\textcircled{D}$  and  $G_i$  denote the D-type of branching and tangent bifurcations, respectively, corresponding to those of Fig. 6.